Using Digital Image Correlation Method for Measuring Surface Crack Opening Displacement and Surface Crack Propagation and Crack Tip in Alpha-Alumina

Mohsin Abbas Aswad
University of Babylon / Materials Engineering
m_a_a_1978@yahoo.com

1-Abstract

There are many techniques were used to measure and observe the surface crack length and surface crack opening displacement (SCOD)at the macro scale but in this study the digital image correlation technique (DIC) is used to measure and obtain the cracks at micro scale and to observe the crack tip. There are many cracks within the microstructure that created during Vickers indentation. The possibility of determining surface crack opening displacement and surface crack length and crack tip in alpha- alumina and determining strain opening using digital image correlation. Due to the anisotropy of crystalline grains that will create residual stress during processing, polycrystalline materials deform and fracture in-homogeneously on a microstructural level.Digital image correlation has sufficient spatial resolution to measure intergranular crack propagation and the crack tip and the surface crack opening in alpha-alumina. The cracks tip are visualized by their stain map but they are not clear on the scanning electron microscopy and optical images, which can be used to measure crack length and surface crack opening displacement. The (SCOD) was calculated using DIC and the minimum SCOD was measured using DIC about 0.05µm at applied stress (30 Mpa).

Key words: Digital Image Correlation, Surface crack length, Crack propagation, Crack tip, Surface crack opening displacement, Strain opening, alumina.

٢ – الخلاصة

هنالك العديد من التقنيات التي استخدمت لقياس طول وعرض الشقوق السطحية على المستوي العيني لكن باستخدام تقنية التصوير بالارتباط الرقمية يمكن حساب طول وعرض الشقوق السطحية على المستوي المايكروي وكذلك لملاحظة حافة الشق. هنالك لعديد من الشقوق تظهر على البنية المجهرية وذلك عند اجراء اختبار فيكرز. فان احتمالية حساب مقدار عرض الشقوق السطحية وطولها وحافة الشق في نموذج الالومينا لطور الفا وكذلك حساب مقدار الانفعال لهذه الشقوق باستخدام تقنية التصوير بالارتباط الرقمية. بسبب عدم الانتظامية للحبيبات البلورية (اختلاف الاتجاهات البلورية) والتي تسبب نشوء الاجهادات المتبقية خلال عملية التصنيع وتشوه البلورات المتعددة يودي لحدوث الكسر الغير متجانس على المستوى البلوري. تقنية التصوير بالارتباط الرقمية لها الدقة العالية لقياس تطور او تقدم الشقوق السطحية الحبيبية وحافة الشقوق وكذلك لقياس عرض الشقوق السطحية في الالومينا ذات طور الفا. تم روية الشقوق من خلال صورة الانفعال لكن هذه الشقوق تكون غير واضحة في صور المجهر الالكتروني الماسح والمجهر الضوئي والتي من خلال صورة الانفعال يتم احتساب طول وعرض الشقوق السطحية باستخدام تقنية التصوير بالارتباط الرقمية اقل قيمة لعرض الشق تم احتسابها بهذه التقنية كانت بحدود (٠,٠٥ مايكرومتر) عند اجهاد مسلط (30 Mpa).

الكلمات المفتاحية: ارتباط التصوير الرقمي، طول الشق السطحي، تقدم الشق، حافة الشق، عرض الشق السطحي،عرض الانفعال، الالومينا.

3-Introduction

The preferred location for cracks is to create on the material surface under bend mechanical loading. Such cracks can be initiated from a wide range of sources of external damage.In many industry fields, alumina ceramic parts are used and they applied successfully. The cracks are readily initiating on the alumina surface during grinding and theses cracks affect the surface quality.The residual stress on the ceramic surface plays important role in the unexpected fracture of ceramic segments and in their dependability in service term. Furthermore, the effects of surface residual stress on fracture toughness of ceramic segments are important,too (Tian,2004 and Jinchuan, 1996).

The kind of crack in alumina ceramic is principally intergranular fracture mode.The crack growing follows not straight path, intergranular path intact grain to bridge the crack faces that resist or prevent the crack opening(Fang,2004).In polycrystalline alumina, the crack between each single grain is more complicated due to influences grain boundaries in alumina and this effect is not present in individual crystal form.Residual stress effects, randomness of grain orientation, constraints from surrounding grains,etc. are represented issues or difficult that evident with polycrystalline alumina (Fang,2004).

By using optical observation, the digital image correlation DIC permits full field strain data to be obtained in every deformation part in materials. The small area in following image that is correlated with multiple interrogation widows these interrogation windows made using digital image correlation operates (Jivkov,2006 and Jivkov, 2008). For each interrogation window, there are displacements vectors can be obtained by the change in the position for this interrogation window. This allows the strain distribution across the full image to be measured (McKenna,2002). There is for each interrogation window size employed a displacement vector accuracy and while larger windows provide for more accurate measurements and there is a decrease in the strain map spatial resolution. For example if the size of interrogation window is 32 × 32 pixels that means the accuracy of calculated is 0.05 to 0.2 pixels but if the window is 128 × 128 pixels the accuracy is 0.01 to 0.03 pixels (Da Fonseca, 2005). Theoretically, this allows measurements accurate to sub pixel displacement for samples that have a random homogenous speckle pattern and where the only change in the image obtained is due to displacement (LaVision,2006). This technique is independent of scale that means the displacement vectors are fixed in pixels and the quality of the results depends on the image quality.

The aim of this paper is to observe, in-situ, the interaction between microstructure and damage development and to evaluate the capability of digital image correlation technique (DIC) in the observation of surface crack length, crack propagation,crack tip, surface crack opening displacement and strain opening.

4-Experimental Work

In this section the crack behavior of the alumina is considered. The crack was created using Vickers indentation and then the load was applied using four points bending rig. The crack behavior was studied using Digital image Correlation.

Digital image correlation requires a random pattern of surface features for optimal displacement vector calculation. This was achieved by grinding and polishing the surface. Then the sample was put inside the furnace at temperature below the sintering temperature(1600^{o}C) about ($150–200^{o}$C).The sample was kept at the thermal temperature etching about (10 hrs.). The alumina sample was coated by gold coating sputtered using an Edwards S150B sputter coating and the time exposure of about 3 minutes. The thickness of this layer depends on the time exposure for the gold coating. The sample had been treated by thermal etching to add some features on the surface. The alumina surface was treated using gold coating was making the surface more applicable for digital image correlation process as shown in Figure1.

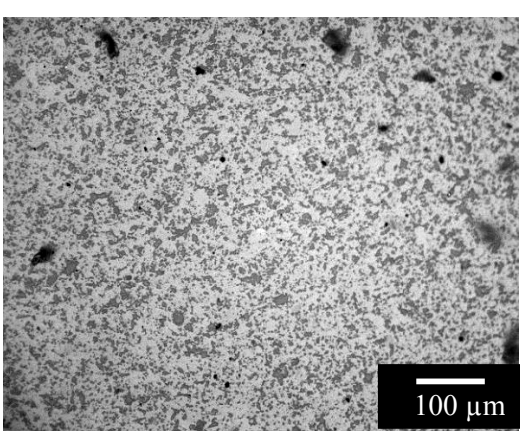

a)

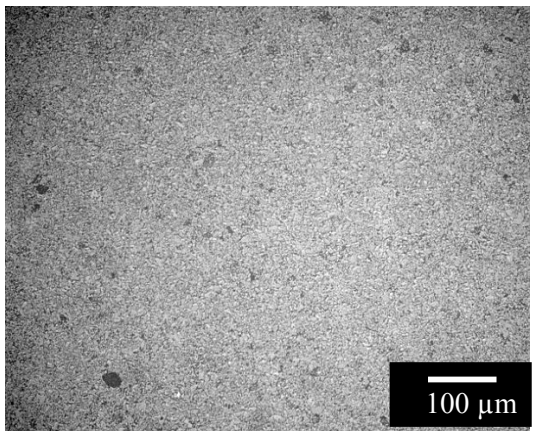

b)

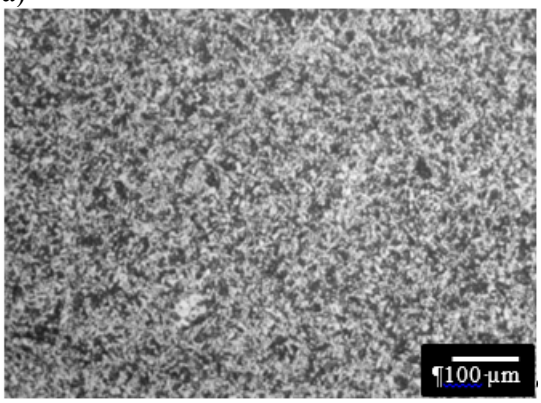

c)

Figure 1: Surface of alumina sample, prepared for digital image correlation a) the polished surface only b) the thermal etched surface c) the gold coated surface after the polishing and thermal etching.

From Figure 1 the sample surface was prepared for digital image correlation. Image (a) the sample was polished only using diamond paste and colloidal silica. Image (b) the sample etched after polishing and the image (c) the sample was coated by gold and the sample surface in this case was more sensitive for the digital image correlation because there are more features on the surface as shown in Figure 1c.

An alumina sample of dimensions (2mm thick, 48mm long and 10mm wide) was used as shown in Figure 2. The surface was ground by using a grinding machine at different grade of diamond wheels (75, 40, 20, 10µm). After that, the surface of sample was polished by using a diamond paste polishing machine at two grades (6 then 1µm).The polishing process took one hour at each grade and then the surface finishing was examined under the optical microscope. After that, the surface of sample was polished by using colloidal silica to remove the small scratch from surface and through this process; the applied pressure, which is used for grinding and polishing.

The strain gauge was fixed on the center of the sample surface in Figure3. The strain gauge diameter was used to measure the strain value about 2 mm. The strain gauge resistivity was used about 120 Ω. It was calibrated using software LabVIEW SignalExpress before the experiment.

Indent was created by using Vickers indentation 10 Kg on the sample surface. Vickers indent created crack on the sample surface. The crack tip was put under the optical microscope image (viewed area) and the viewed area was recorded at different applied loads subsequently. Digital image correlation was used to assess optical images of the cracked sample, recorded under variable loads. The objective was to

assess the sensitivity of displacement measurement in this sample, and hence its ability to record crack propagation.

The four point bending sample was conducted with the strain gauge to measure the strain on the sample surface after the sample was deformed at each 5 min. A loading rate was increased by using micrometer to apply the load in the X-direction and the crack growing was normal on the loading direction as shown in Figure 1. The sample surface was imaged via an Olympus CH-2 optical Microscope with X20 lens and with the working distance about 38mm. The images were recorded with a Zeiss MRm digital camera (14 bit, up to 14 frames/second, 1300×1300 pixels).Digital Image Correlation was then carried out on a networked Dual Processor PC (2×2.8 GHz Processors, 2 Gb RAM), with Davis Strain Master 2D software for acquisition and visualization,(LA Vision, Germany). With X20 objective lens, the field of view is approximately 576µm×450µm.Figure ٢ shows the digital image correlation technique and fracture test setup.

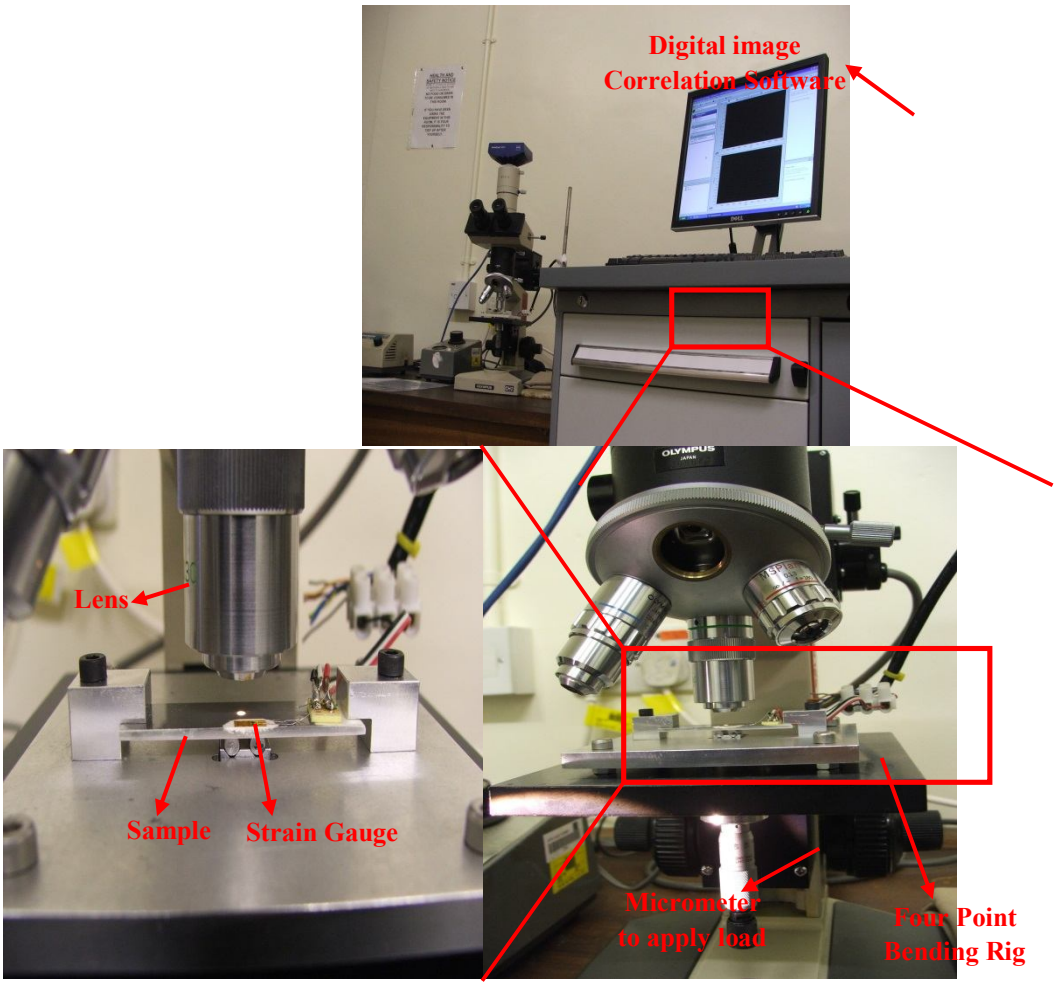

Figure 2: Digital image Correlation equipment. Loading rig for in-situ image correlation of the tensile surface during four-point bent loading with friction minimised by free movement of the loading pins. A specimen is shown in enlarged image.

Before the load was applied, the digital camera took the initial image without deformation (initial image).The displacement was incremented by 0.02mm at 30 min intervals. Through this time, the digital camera took image at each 5 min. at the same load. Seven images were taken at each increment. Typically, four increments were reached to break the sample.

5- Results and Discussion

5-1 Uncertainty in displacement vector magnitude

Interrogation window size is known to have an effect on the accuracy of the calculated displacement vector,with the increased number of surface features included in larger window sizes decreasing correlation uncertainty. For this work, uncertainty was assessed by the images of the sample with a small applied rigid body displacement between them were collected and displacement vectors calculated. All calculated vectors should be identical, with any spread being due to noise in the displacement vector calculation or experimental error. The analysis is based on a single pass at a fixed window size and smaller windows tend to give higher displacement noise. For an interrogation window size of 128×128 pixels and one pass, the standard deviation of the calculated displacement vectors was 0.031 μm (i.e. 0.013 pixels).

Comparing between the interrogation window size 128×128 pixel and 64×64 pixel. The overlap for both interrogation window sizes was 75%. The uncertainty for interrogation window size 64×64 pixel was 0.02 to 0.05 pixels but the uncertainty for interrogation window size 128×128 pixel was 0.01 to 0.03 pixels (LaVision and DaVis,2006). Figure 3 shows the interrogation windows size were used to measure the displacement and the plot for the window size 128×128 is much smoother which is used to measure the displacement.

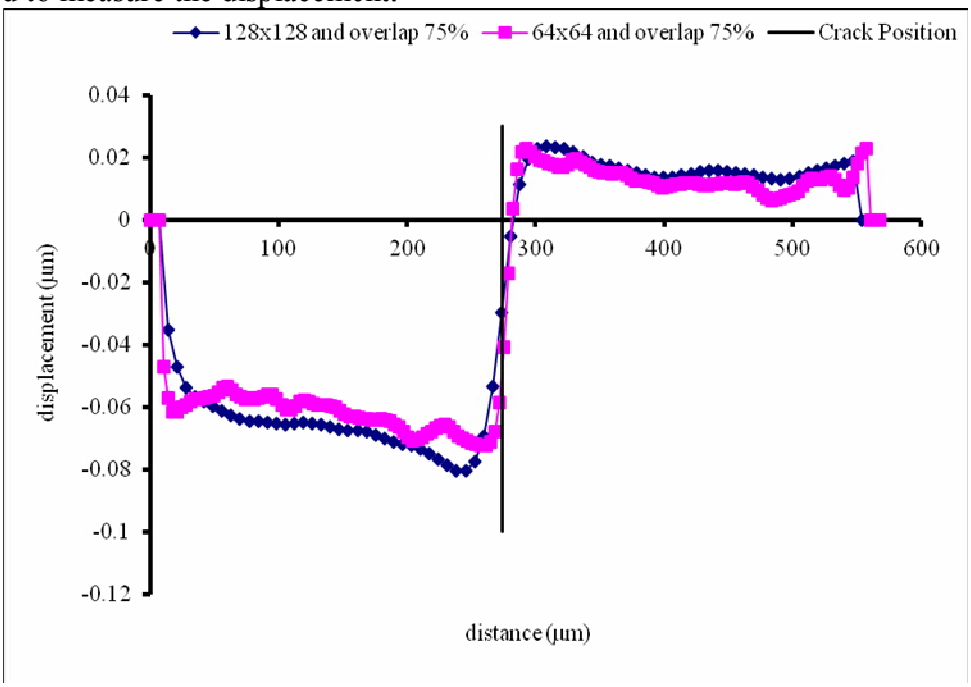

Figure 3: Interrogation window sizes of 128 × 128 and 64 × 64 are compared. The location of the crack plane is shown (normal black line).

5-2 Initial Image Correlation Analysis

Digital Image Correlation, DIC was performed on the image sets, using window sizes of either 128 × 128 pixels or 64 × 64 pixels. The maximum overlap of 75% was used to provide a high density of displacement vectors. An image of the X-direction displacements is shown in Figure 5 for the sample loaded at 70 MPa and with a window size of 128×128 pixels.The X-direction is perpendicular to the crack and parallel to the applied tensile load.

The crack was observed at each increment and it was quite clear on the strain map as shown in Figure 4.The colour contours indicate the number of images in which cracks were identified at each position. Optical images of the sample solution

taken at (4 hrs.).The stress axes in the horizontal (X-direction) and the small curvature of the specimen, while under load, had no effect on the image quality. Analysis by DIC reveals localized regions of high strain parallel to the X-direction. Strain maps in Figure 4 show these high strain regions and the crack growing. Therefore, these high strain regions were designated as cracks.

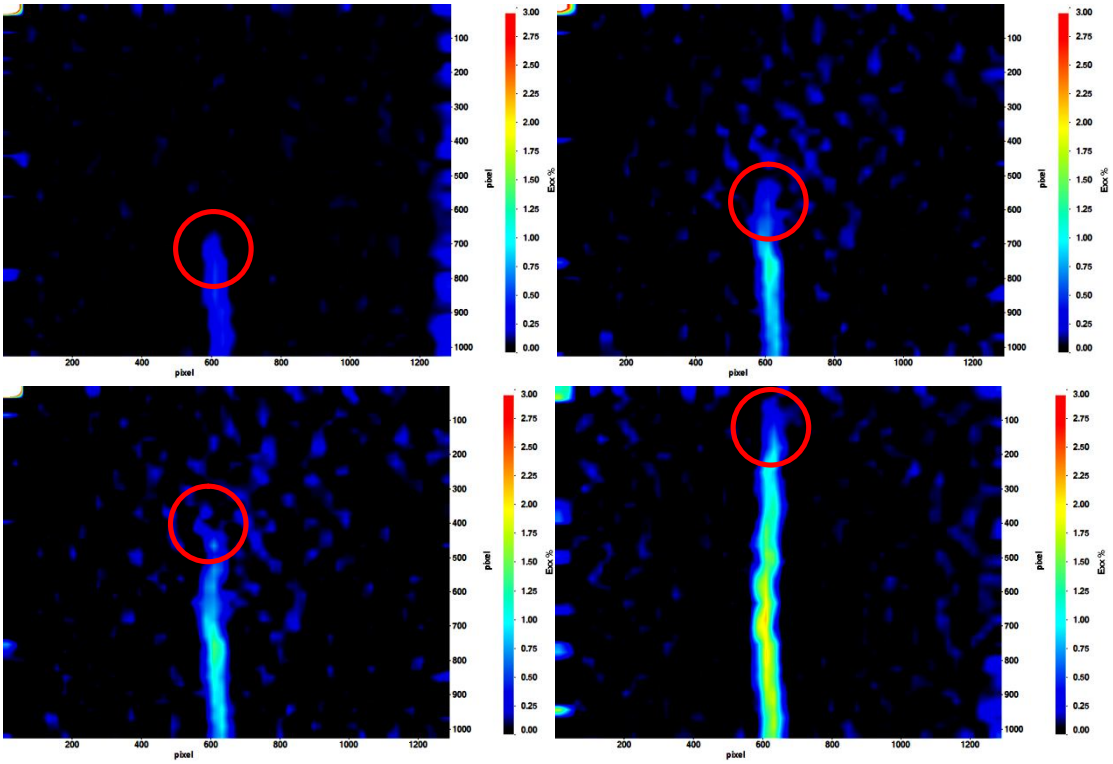

Figure 4: Illustration of the increase in crack length and strain distribution observed by image correlation under increasing load, the red circles show the crack tips of the crack propagation.

The image correlation data identified the features using strain map. Strain map is a result of the measured relative displacements of material on either side of the feature. The magnitude of the strain depends on the differentiation of this displacement (Hack,1980).The strain data were analyzed to determine the maximum strain measured with each feature. High strain regions corresponded well with the location and length of the cracks. These strain features are surface cracks but proportional measure of the maximum crack opening displacement, as a function of crack surface length and applied load as shown in Figure 4.

The colour contour indicates the number of images in which cracks were identified at that position, with blue (dark) being the highest number. Crack growth occurs through both extension of the small crack and through the coalescence of the small cracks in front of the crack tip. From Figure 4 the crack growth was increased for each load increment and the background for each image is different because the focus was changed at each time. That means the strain noise for the images (b and c) was too much because the focus is changed. In image (d) the surface crack length was increased suddenly due to the increasing the load that means the small cracks coalescence which gave an increased crack length. The crack growing and opening were observed easily by DIC as shown in Figure 4 but they could not be observed by optical microscope.

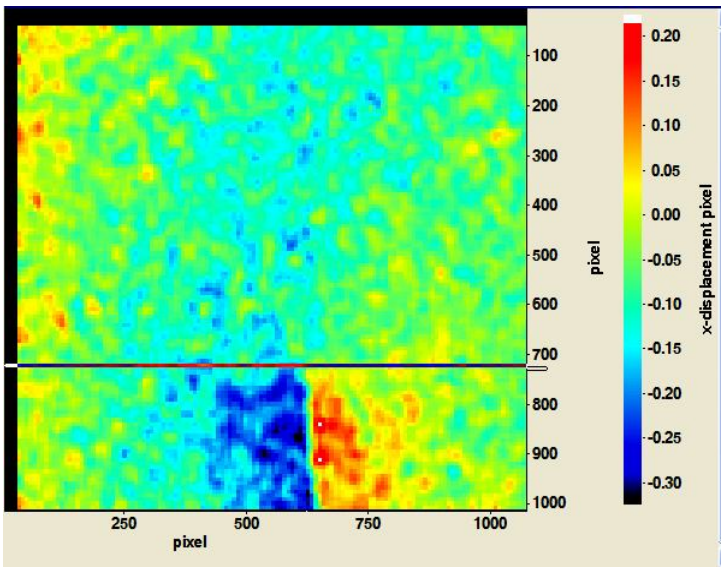

Figure 5: Displacement map in the X-direction for the sample loaded at 70 MPa. The interrogation window size is 128×128 pixels with an overlap of 75%.

A set of displacement profiles (for displacement parallel to the x-direction) are shown in Figure 6 at selected positions for the sample loaded at 70 MPa. The crack tip is located at the position at 550 µm, so three of the profiles are across the open crack and two are located ahead of the crack tip. Locations of the five line profiles are shown in Figure 7. The centre line of the crack is 274 µm from the left of the image. As the sample is loaded a displacement gradient develops. The opening of the crack is characterised by a step change in the profile.

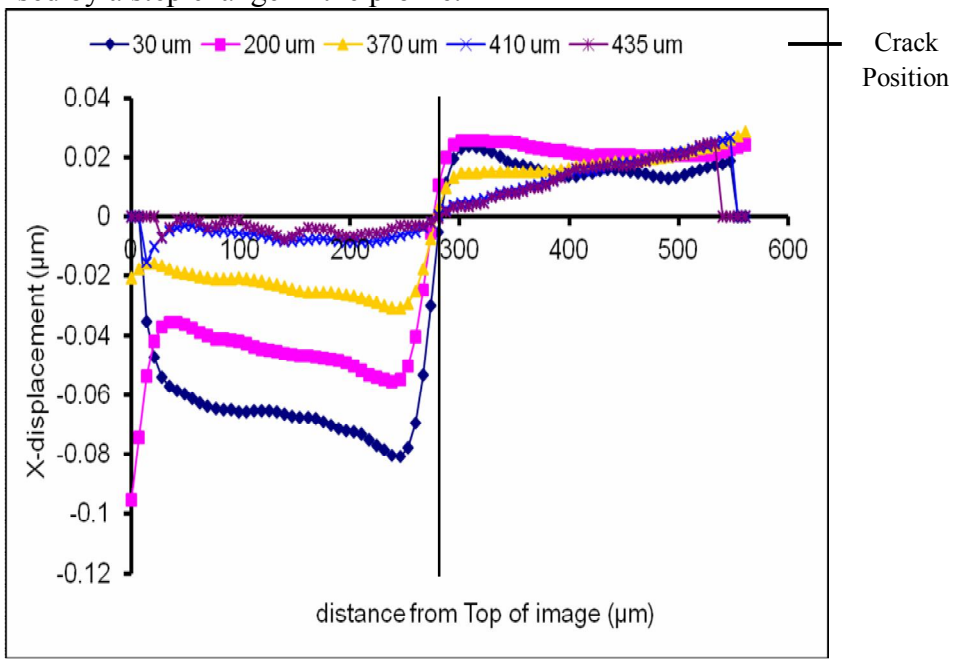

Figure 6: X-Displacement Line Profiles at selected positions along image height.

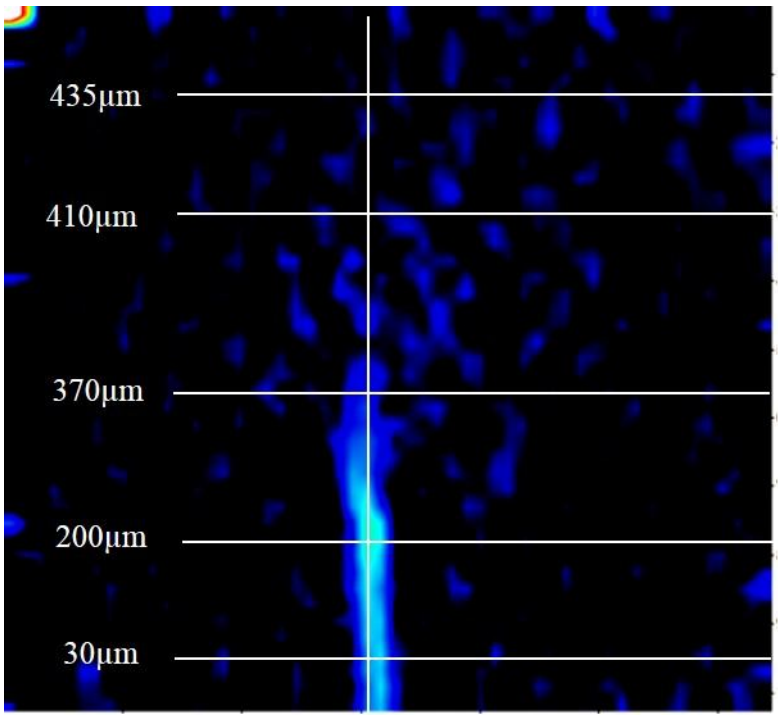

Figure 7: Location of line profiles plotted in Figure 6. Distances are measured from the top of the sample. The crack tip is at 550 µm. The crack centre line is 274 µm from the left of the image.

5-3 Crack Growth Behavior

The data were obtained for the variation of measured surface crack length at different applied stresses (30, 50, 70, 90 MPa) against the time as shown in Figure 8. The applied stresses were measured from strain gauge. The crack growth behavior was measured as mentioned in section 5.2.3 in Figure 4, image (J) was used to measure the surface crack.

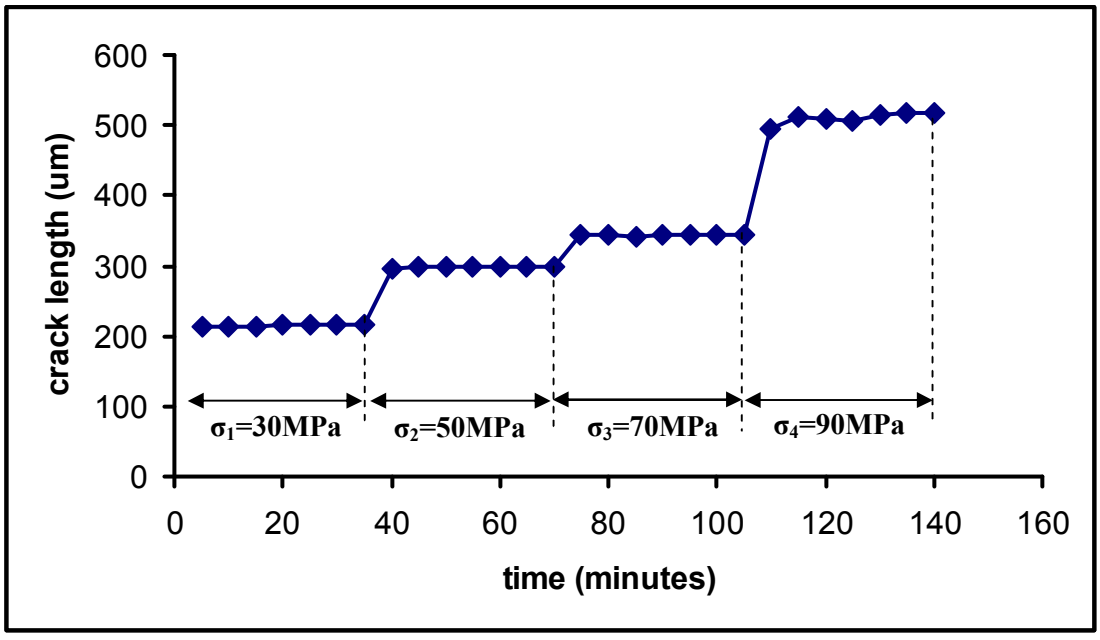

Figure 8: Development of surface crack lengths at different applied stresses against the time.

From Figure 8 there was little increase the crack length for each stress increment and the crack growth occurred with increasing strain. At the fourth increment the

crack length increased suddenly due to the crack coalescence with small cracks and increased applied load on the sample surface.

5-4 Measurement of the crack opening

The surface crack opening displacement was measured by different methods as shown below:

5-4-1 Using Model

The surface crack opening displacement (SCOD) was measured at different applied stresses using Equation 1 [9].

$$SCOD = 4\sqrt{2} \times (1 - \nu^2) \times \left(\sigma \times \frac{a}{E} \right) \qquad \textbf{(1)}$$

Where: ν= Poisson Ratio for alumina (0.22) [10], σ = the applied of stress (Mpa), a=crack depth (300μm), E = Young's modulus (350Gpa) (matweb, website).

The typical crack depth was determined by polishing an indented sample with a crack until the crack had been removed and the crack depth was (300μm) using optical microscope. The calculated SCOD increased at each applied stress due to an increase in crack depth. The results for SCOD and noise level or accuracy was about (0.039 μm) have been shown in Figure 9.

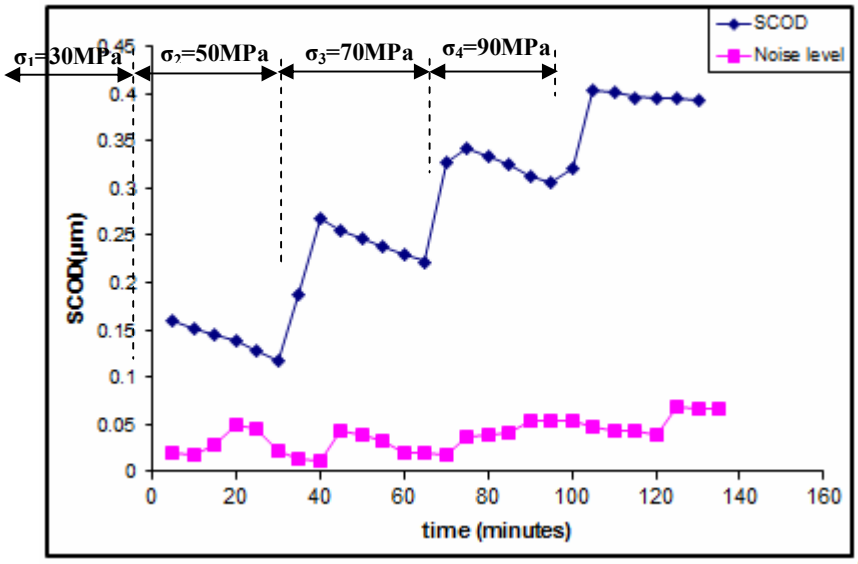

Figure 9: Development the predicted SCOD versus time. SCOD was compared with the noise level or accuracy as mentioned in section (5-1).

From Figure 9 the SCOD was measured using Equation 1 and the SCOD was increased at each applied stress. The maximum crack opening displacement depended on the crack geometry and loading, is given in Equation 1. The red curve shows the noise level in the displacement image and their data on whole test were lower than displacement data on the each side of the crack as shown in blue curve. The SCOD curve was higher at each applied load and then SCOD curve relaxed due to the alumina was elastic materials.

5-4-2 Using Window on each side of the crack

The SCOD increased with increasing the crack length at each applied stress. This would be observed as an increase in the magnitude of strain. It is noted that in bending test the SCOD might be increased by the bending moment. The values of the surface crack opening displacement at different applied stresses were higher than the noise level as shown in this Figure10b.

The SCOD was also measured using Davis version7.2 software. The displacement vector data were exported on each side of the crack as shown in Figure 10a. A single average displacement vector was formed for each rectangle and the displacement for the left hand side (LHS) rectangle was subtracted from the displacement for the right hand side (RHS) rectangle to get the surface crack opening displacement and the SCOD results as shown in Figure 10b.

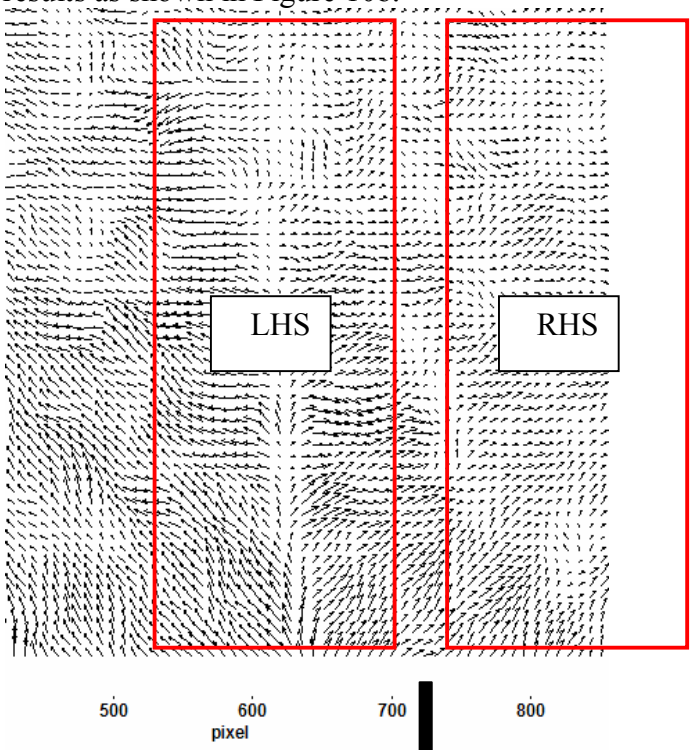

a)

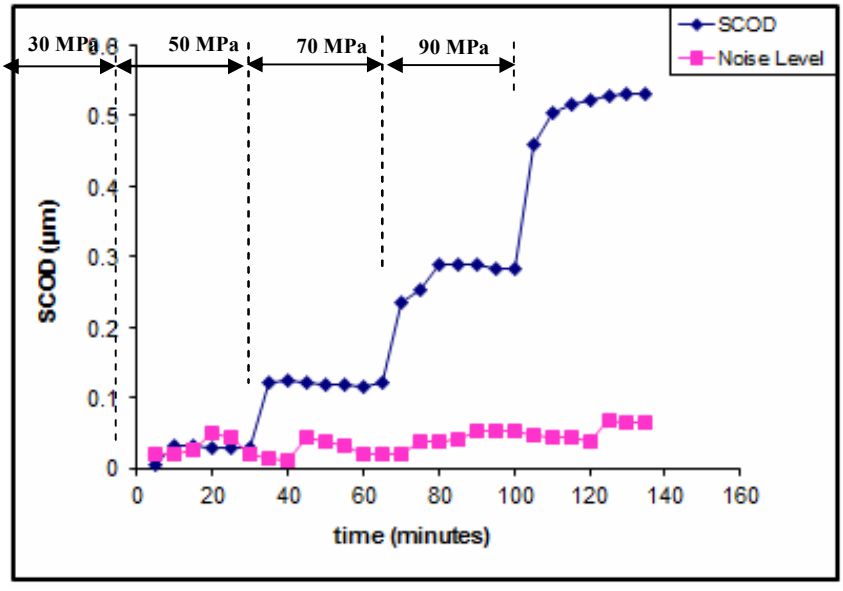

b)

Figure 10: a) The SCOD was measured for all the data using Davis b) Development the SCOD versus time at different applied stresses.

The measured SCOD was determined by the subtracting the displacement on the RHS from the displacement on the LHS (i. e. SCOD=RHS (displacement)–LHS (displacement)) and the results as shown in Figure 10b.

5-4-3 Using Line Profile along the crack length

Using Davis version 7.2 at different applied stresses from the distance behind the crack tip as shown in Figure 11. The data were exported from Davis software to Microsoft Excel to measure SCOD at different applied stresses and distances from the crack tip to the crack bottom. The results have been shown in Figure 12.

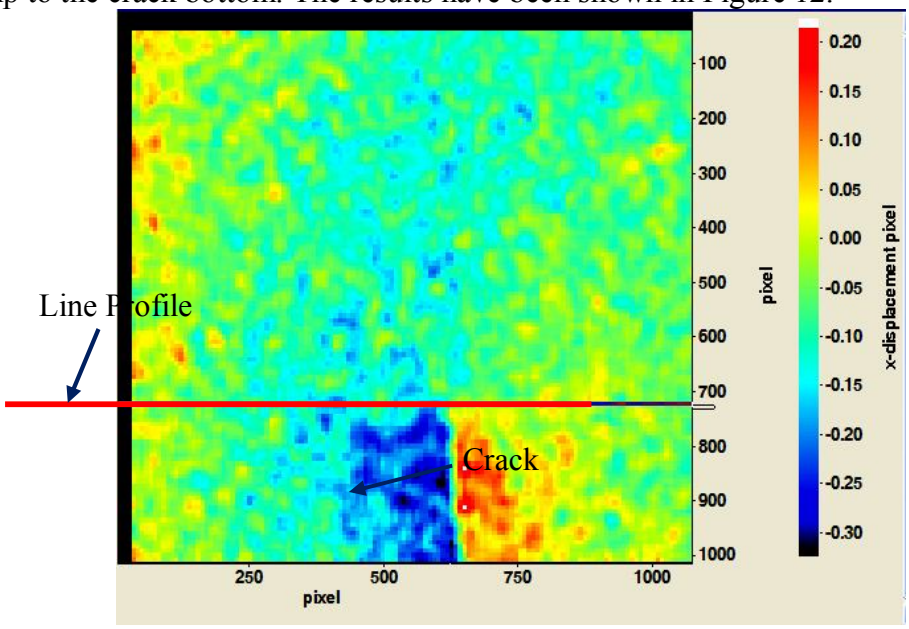

Figure 11: The SCOD was measured behind the crack tip at different applied stresses and distances.

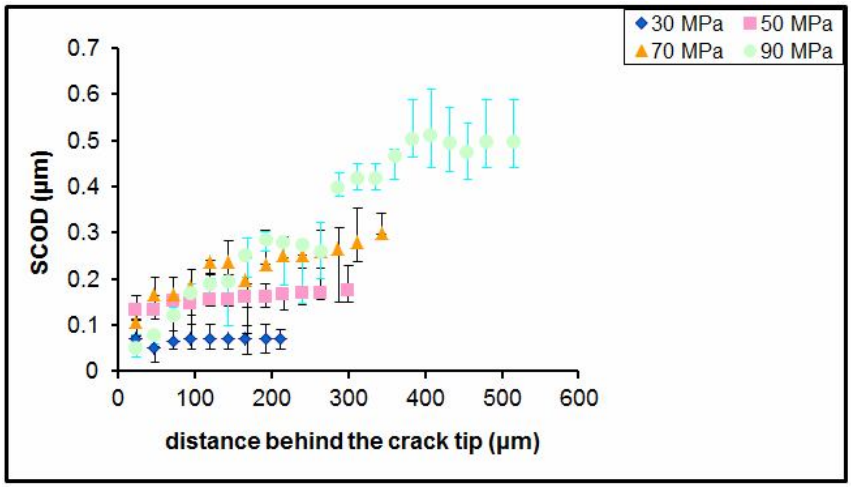

Figure 12: Development the SCOD versus the distance behind the crack tip (as shown in Figure 11) from Davis at different applied stress.

The relationship between the surface crack opening displacement and the displacement behind the crack tip is represented in Figure12.The surface crack opening displacement tends to increase with increasing the surface crack length. At each applied stress the surface crack opening displacement behind the crack tip increased also.The crack expanding from the crack tip until the bottom of the crack.That means the highest surface crack opening displacement at the crack bottom as shown in Figure 12.

The digital image correlation technique is sensitive to observe the crack in alumina. That means the minimum surface crack opening displacement was observed

about 0.05μm at the minimum applied stress (30 MPa) was determined using digital image correlation.

5-5 BreakPoint analysis method

The break in the displacement profile due to the crack opening is not necessarily large, particularly close to the crack tip (Figure 13), but it affects the rest of the displacement profile and can be detected using a break point algorithm (Equation 2) (Hawkins,1977), *BP* is the breakpoint intensity at position *n* in the line profile, Av_1 is the average value of the displacement for a set number, *MA,* of positions before *n,* Av_2 is the average value of the displacement for *MA* positions after *n,* and Av_{All} is the average displacement over the whole range. As the breakpoint intensity is normalised by the standard deviation of Av_{All} localised noise is not misinterpreted as crack opening.

Equation 2 – Local Breakpoint intensity

$$BP_N = MA\frac{(Av_1 - Av_{All})^2 + (Av_2 - Av_{All})^2}{STD_{All}}$$

Crack opening can be calculated using Equation 3, applied to the displacement profiles. The Crack opening at position *n*, is equal to difference between the average displacements at positions below *n* and above *n*.The number of average displacements, *MA,* was calculated with an offset value, *off,* added to take account of the gradual change in vector displacement across the crack. This equation was applied down the length of each vector column with the largest crack opening indicating the full crack opening for that column.

Equation 3 – Crack Opening

$$CrackOpening_n = \frac{\sum_{i=n-off-MA}^{i=n-off} Ydisp_i}{MA} - \frac{\sum_{i=n+off}^{i=n+off+MA} Ydisp_i}{MA}$$

A comparison of the outputs that the BreakPoint calculation and the CrackOpening calculation have on an individual line profile is shown in Figure 13. For the BreakPoint algorithm, *MA* was 6 and in the Crack Opening algorithm, *MA* was 6 and *off* was *6*. These values were determined by judgement, based on visual inspection of the displacement profiles shown in Figure 13. The data are compared with the BreakPoint intensity, the X-displacements across the crack and the known position of the crack plane

Differentiation with respect to distance, using the results produced by Equation 2, can be performed producing a smoothed x-direction strain profile. Localised strain behind of the crack tip can be identified in images and the strain ahead of the crack tip is negligible. The position of the crack tip is quite well identified.

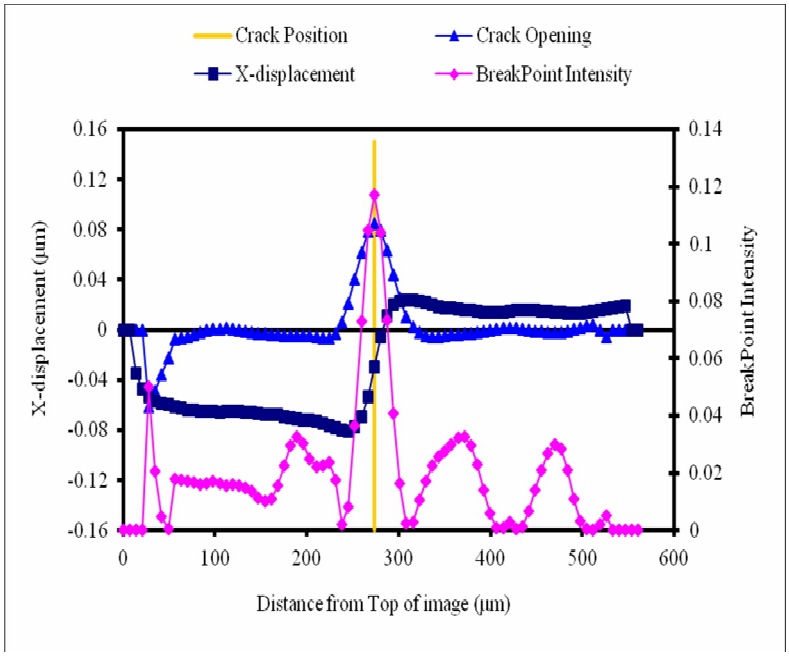

Figure 13: Example of the BreakPoint and Crack Opening Output for X-Displacement for the line profile across the crack at 1600 µm from the sample edge.

6- Conclusions

1) The main crack path was obvious but the crack tip is difficult to observe using optical microscope.
2) The digital image correlation was used to observe the crack tip.
3) The high strain regions correspond to the crack length and it was quite clear on the strain map.
4) The crack propagation increases with increasing the applied stress due to the crack coalescence at each increment.
5) The minimum surface crack opening displacement was measured by digital image correlation about 0.05µm at the first increment at minimum load 53.1N.
6) The opening strain was measured using digital image correlation.
7) The digital image correlation is sensitive to show an observe the crack tip at different loads increment.
8) The digital image correlation was used to measure surface crack opening displacement at micro-scales.
9) The break point was used to detect the crack opening close to the crack tip in the displacement profile due to the crack opening is not necessarily large, particularly close to the crack tip

7- References

Da Fonseca, J.Q., Mummery, P. M., and Withers, P.J., 2005, Full-field strain mapping by optical correlation of micrographs acquired during deformation. Journal Of Microscopy-Oxford. 218: p. 9-21.

Fang,Y.,Fossier,T., and White, K.W.,2004,Crack path simulation and identification in polycrystalline alumina. Scripta Materialia. 50(1): p. 127-130.

Hack, J.E.,and Leverant,G.R.,1980,On The Prediction of the Surface Crack Opening Displacement of a part through Crack. Int Journ of Fracture, USA.

Hawkins,D. M.,1977, Journal of the American Statistical Association, Vol. 72, No. 357 (Mar.), pp.180-186

http://www.matweb.com/search/PropertySearch.aspx, Material Property Data.

Jinchuan,Z.Z.1996,Advanced Cutting and Grinding Technologies of Brittle Materials. U.S.: Oxford Science Press.

Jivkov,A.P.,Stevens,N.P.C.,and Marrow,T. J.,2006,A two-dimensional mesoscale model for intergranular stress corrosion crack propagation. Acta Materialia 54(13): p. 3493-3501.

Jivkov, A.P.,Stevens, N.P.C.,and Marrow,T. J.,2008, Mesoscale mechanical model for intergranular stress corrosion cracking and implications for microstructure engineering. Journal Of Pressure Vessel Technology-Transactions Of The Asme. 130(3).

LaVision, DaVis Strain MasterMaster Softerware Manual 7.1.:2006, LaVision GmbH, Gottingen.

McKenna,S.P.,and McGillis,W.R.,2002,Performance of digital image velocimetry processing techniques. Experiments In Fluids. 32(1): p.106-115.

Tian, X.L.andYu, A.B.,2004,Change of residual stress after grinding Al2O3 ceramics, in Advances In Grinding And Abrasive Processes, Trans Tech Publications Ltd: Zurich-Uetikon. p. 481-484.